Angle-resolved photoemission and the electronic structure of Pd(111)

Ralf Hora and Matthias Scheffler
Physikalisch-Technische Bundesanstalt, Postfach 3345, D-3300 Braunschweig, Federal Republic of Germany
(Received 13 September 1983)

A theoretical study of various models which are commonly used for the analysis of angle-resolved photoemission is reported. For the example of the Pd(111) surface we discuss the quality and justification of these models. We have calculated the $\vec{k}_{||}$-resolved surface and bulk densities of states and the band structure of occupied and unoccupied states. Furthermore, we have calculated photoemission spectra within the one-step approach. These theoretical spectra reproduce the main features and trends of the experimental data. We find that the $\vec{k}_{||}$-resolved densities of states are, in general, not reflected in the photoemission. The spectra can only be interpreted in a *modified* direct-transition model where the influence of the inelastic electron-electron interaction in the final state is taken into account.

I. INTRODUCTION

Angle-resolved ultraviolet photoelectron spectroscopy (ARUPS) has become a common technique for investigating the electronic structure of clean and adsorbate covered surfaces.[1] The success of this method is largely due to its high surface sensitivity (the escape depth of elastically photoemitted electrons is of the order of 5—10 Å) and to the fact that the experimental data can be interpreted nearly completely in terms of a single-particle picture. In applications to ordered adsorbate layers the method allows a direct experimental determination of the two-dimensional band structure $E(\vec{k}_{||})$ of the adlayer induced states.[2] On the other hand, for clean surfaces the method has been used not only to extract information about surface states, but also for an experimental determination of the three-dimensional bulk band structure.[3—7] In contrast to the analysis of surface features we note that those interpretations in terms of a bulk band structure are not only based on experimental data, but they also rely on theoretical models. Unfortunately these models depend on several assumptions of which the justifications are still open. Often different authors use different models for their analysis of experimental data. For clean crystals, ARUPS is mostly interpreted in terms of the three-step model of photoemission.[8] In this approximation the excitation should happen sufficiently far from the surface and should not be affected by it. Furthermore the three processes of (1) excitation in the bulk, (2) transport of the excited electron to the surface, and (3) transmission into the vacuum are assumed to occur independently from each other. Despite the success of this approach for interpreting experimental spectra, a detailed understanding of its justification is still missing. The main problem with this approach arises because it assumes that all three components of the electron wave vector $\vec{k}$ are good quantum numbers, that they are known and conserved in the excitation process. This is certainly true for the components of $\vec{k}$ parallel to the surface (k_x,k_y) because the symmetry is conserved in these directions. However, perpendicular to the surface the symmetry is broken. In turn the component k_z is not a good quantum number. Even if there were an approximate validity of the three-step model, k_z is not conserved upon the transmission of the photoelectron into the vacuum. As a consequence, the determination of k_z—which is the needed normal component of the wave vector *inside* the crystal—remains an important problem. Several methods which allow a pure experimental determination of k_z have been developed (see, e.g., Ref. 9, and references therein). Unfortunately these methods are not always applicable and even if they are, the determination of k_z is often not conclusive. Therefore, most published work is based on other methods which rely on further theoretical assumptions introduced even on top of the three-step model. In fact, two different methods have been used in the past. The first approach uses a theoretical bulk band structure of a ground-state calculation.[4—7] In applications of this approach it was found that it can describe most experimental results. However, one shortcoming is obvious: this model gives no emissions at energies and directions which correspond to a band gap of the unoccupied (final) state band structure. This is in clear contrast to the experimental results.[7] The second approach assumes that the final-state band structure can be described by a free-electron parabola, the energy zero of which is used as an adjustable parameter.[3] Peaks in the photoemission spectra are then interpreted in terms of direct transitions between the initial-state band structure ($E \leq E_F, E_F$ is the Fermi energy) and this parabola. The results, i.e., the experimentally deduced initial state bands were in surprising agreement with corresponding theoretical ones.

An alternative approach to the above-mentioned models emphasizes the high surface sensitivity of ARUPS. It is well known that transition metals have a high density of surface states and surface resonances.[10,11] As those should contribute significantly to the photoemission and because k_z is certainly not defined for them, it might be argued that an angle- and energy-resolved photoemission spectrum should be analyzed in terms of the $\vec{k}_{||}$-resolved den-

sity of states at the surface.[11–13]

The most sophisticated approach for analyzing ARUPS, which would also account for all above-mentioned models, if they were valid, is the one-step theory. In this approach the energies and wave functions of the semi-infinite crystal are calculated and the photocurrent is evaluated from the golden-rule formula [see Eq. (3) below]. For clean surfaces the first calculations of this type were performed by Pendry and Titterington[14] and by Jepsen.[15]

In this paper we address the questions of quality and justification of the various models which have been used for the interpretation of ARUPS on clean crystals. For this purpose we have performed a variety of calculations using an approach which is based on the two-dimensional Korringa-Kohn-Rostoker (KKR) method.[16,17] As a first step we have calculated angular-resolved photoemission spectra for the emission from a Pd(111) surface. We compare these results to experimental data in order to show that these calculations reproduce indeed the main experimental results. Unfortunately and despite the fact that those calculations are quite elaborate, the comparison of theoretical photoemission spectra with the experimental ones allows no deep insight into the nature of the photoemission process and it also gives no direct justification of one or another of the above-mentioned models. Therefore, we have also studied these models and we compare them with the calculated photoemission spectra. In particular we investigate the $\vec{k}_{||}$-resolved density of occupied states at the surface and in the bulk. We find that structures in those local densities of states are in general not related to the features of the corresponding photoemission spectra.

Furthermore, we study the bulk band structure at the initial- and final-state energies. Here we find that a simple direct transition model where the initial- and final-state bands are calculated with the same (ground-state) potential, in general, cannot account for the structures in photoemission spectra. It is shown that the effective single-particle potential of the ground state needs to be modified for excited electrons. In particular the inelastic electron-electron interaction has to be taken into account as it affects the dispersion of the bands by dehybridization and even energy gaps can be closed. The theoretical analysis shows that the angle-resolved photoemission can be understood in terms of a direct transition model if the inelastic electron-electron interaction in the final state is taken into account. Further, this analysis gives a justification of using a free-electron parabola for the dispersion of the unoccupied band structure in the analysis of angular-resolved photoelectron spectra. We note, however, that the wave function of the excited state deviates significantly from a single plane wave.

In the following section we discuss the theoretical background of our study. In particular we describe the method for calculating the $\vec{k}_{||}$-resolved Green's function of a semi-infinite crystal. Section III then deals with the comparison to experimental data and with the theoretical investigation of models which are commonly used for the analysis of ARUPS from a clean surface.

II. THEORY

This section deals with the theoretical background and the method of our study. In particular we describe the calculational approach to evaluate the $\vec{k}_{||}$-resolved Green's function for a semi-infinite crystal. Further, we address the calculation of the excited-state energy bands and wave functions. Finally, we give the parameters which enter the actual calculations of the Pd(111) surface. Hartree atomic units are used.

In the one-electron approximation the energy- and angle-resolved photocurrent is given by the golden-rule formula:

$$I(E_f,\theta,\phi)=\frac{1}{16\pi^3}(2E_f)^{1/2}\sum_i^{\text{occ}} |\langle f|H'|i\rangle|^2 \times\delta(E_f-E_i-\hbar\omega) . \quad (1)$$

Here E_f is the energy of the detected electron and θ is the polar angle of the detector position measured with respect to the surface normal. Correspondingly, ϕ is the azimuthal angle defined with respect to the x and y axes in the surface plane. The operator of the photon-electron interaction is $H'=(1/c)\vec{A}\cdot\vec{p}$, with $\vec{A}$ as the vector potential, $\vec{p}$ as the momentum operator, and c the velocity of light. Thus we neglect the spatial dependence of the electromagnetic field inside the crystal. However, we take into account the refraction of the light at the surface and we determine the vector potential in the crystal according to the Fresnel formula. The sum in Eq. (1) covers all occupied states. The energy of the ultraviolet light is $\hbar\omega$. The time-reserved final state $\langle f|$ satisfies the same boundary conditions as a low-energy electron diffraction (LEED) wave function.[18] Thus it is the scattering solution for an electron incident from the position of the detector onto the crystal surface. As the energy of this electron is E_f, its $\vec{k}$ vector is

$$\begin{aligned} k_x&=(2E_f)^{1/2}\sin\theta\cos\phi ,\\ k_y&=(2E_f)^{1/2}\sin\theta\sin\phi , \quad (2)\\ k_z^{\text{out}}&=(2E_f)^{1/2}\cos\theta . \end{aligned}$$

The index "out" is noted at the z component, because this component is only well defined outside the sample. Because of the periodicity parallel to the surface, the wave function $|f\rangle$ satisfies the two-dimensional Bloch theorem. Therefore, k_x and k_y are well defined outside and inside the crystal (at least modulo $\vec{g}$ where $\vec{g}$ is a two-dimensional reciprocal-lattice vector).

If we replace the sum over occupied states and the δ function in Eq. (1) by the imaginary part of the Green's function, we get

$$I(E_f,\theta,\phi)=-\frac{1}{8\pi^4}(2E_f)^{1/2}\int\int d^3r\,d^3r'\,\phi_f^*(E_f,\vec{k}_{||};\vec{r})H'(\vec{r})\text{Im}[G(E_f-\hbar\omega,\vec{k}_{||};\vec{r},\vec{r}')]H'(\vec{r}')\phi_f(E_f,\vec{k}_{||};\vec{r}') . \quad (3)$$

Here we have also taken into account the periodicity of the semi-infinite crystal. Therefore, $\vec{k}_{||}$—if reduced to the first surface Brillouin zone (SBZ)—is a good quantum number and the Green's function can be written as

$$G(E,\vec{r},\vec{r}\,')=\int_{\mathrm{SBZ}} d^2k_{||}\,G(E,\vec{k}_{||};\vec{r},\vec{r}\,') \,. \tag{4}$$

Because the dipole operator H' does not destroy the translational symmetry parallel to the surface, $\vec{k}_{||}$ is conserved in the excitation process and the integral of Eq. (4) does not appear in Eq. (3). Equation (3) shows that the energy- and angle-resolved photocurrent is not only determined by the $\vec{k}_{||}$-resolved density of states $(-(2/\pi)\mathrm{Im}[G(E,\vec{k}_{||};\vec{r},\vec{r})])$ but the off-diagonal elements of $G(E,\vec{k}_{||})$ enter as well.

A. Layer Green's function

In order to calculate the Green's function of a semi-infinite crystal, which enters Eq. (3), we start from the Dyson equation

$$G(E,\vec{k}_{||};\vec{r},\vec{r}\,')=G^0(E,\vec{k}_{||};\vec{r},\vec{r}\,') + \int d^3r''\,G^0(E,\vec{k}_{||};\vec{r},\vec{r}\,'')V(\vec{r}\,'') \times G(E,\vec{k}_{||};\vec{r}\,'',\vec{r}\,') \,. \tag{5}$$

Here $V(\vec{r})$ is the potential energy of the semi-infinite crystal and $G^0(E,\vec{k}_{||};\vec{r},\vec{r}\,')$ is the vacuum Green's function. It is convenient to use a vacuum Green's function which is already adapted to the two-dimensional periodicity (parallel to the surface):

$$G^0(E,\vec{k}_{||};\vec{r},\vec{r}\,')=\frac{1}{\Omega}\sum_{\vec{R}_j}\frac{e^{i\sqrt{2E}\,|\,\vec{r}-\vec{r}\,'-\vec{R}_j\,|}}{|\,\vec{r}-\vec{r}\,'-\vec{R}_j\,|}e^{i\vec{k}_{||}\cdot\vec{R}_j}$$

$$=\frac{1}{\Omega}\sum_{\vec{g}}\frac{1}{ik_{g_z}}e^{ik_{g_z}|\,\vec{z}-\vec{z}\,'\,|} \tag{6a}$$

$$\times e^{i(\vec{k}_{||}+\vec{g})\cdot(\vec{r}-\vec{r}\,')} \,. \tag{6b}$$

Here $\vec{R}_j$ span a two-dimensional lattice with the unit cell area Ω. $\vec{g}$ are the corresponding two-dimensional reciprocal-lattice vectors and k_{g_z} is defined as

$$k_{g_z}=\begin{cases}+[2E-(\vec{k}_{||}+\vec{g})^2]^{1/2}, & \text{if } (\vec{k}_{||}+\vec{g})^2\le 2E,\\ +i[(\vec{k}_{||}+\vec{g})^2-2E]^{1/2}, & \text{if } (\vec{k}_{||}+\vec{g})^2\ge 2E \,.\end{cases} \tag{7}$$

In order to solve Eq. (5) we treat the crystal as a system of nonoverlapping layers

$$V(\vec{r})=\sum_{i=0}^{\infty}V_i(\vec{r}) \,, \tag{8}$$

where $V_0(\vec{r})$ is the surface barrier, $V_1(\vec{r})$ is the surface atomic layer, $V_2(\vec{r})$ the second atomic layer, etc. Equation (5) can be rewritten now as

$$G(E,\vec{k}_{||};\vec{r},\vec{r}\,')=G^{e(j)}(E,\vec{k}_{||};\vec{r},\vec{r}\,') + \int d^3r''\,G^{e(j)}(E,\vec{k}_{||};\vec{r},\vec{r}\,'')V_j(\vec{r}\,'') \times G(E,\vec{k}_{||};\vec{r}\,'',\vec{r}\,') \tag{9}$$

with

$$G^{e(j)}(E,\vec{k}_{||};\vec{r},\vec{r}\,')=G^0(E,\vec{k}_{||};\vec{r},\vec{r}\,') + \int d^3r''G^0(E,\vec{k}_{||};\vec{r},\vec{r}\,'') \times\sum_{\substack{i=0\\ i\neq j}}V_i(\vec{r}\,'')G^{e(j)}(E,\vec{k}_{||};\vec{r}\,'',\vec{r}\,') \,. \tag{10}$$

$G^{e(j)}$ is called the empty layer Green's function because it is a Green's function of a semi-infinite crystal where the jth layer is missing. The advantage of Eqs. (9) and (10) compared to Eq. (5) arises, if $G(E,\vec{k}_{||};\vec{r},\vec{r}\,')$ is needed only for $\vec{r},\vec{r}\,'$ within the range of one or another layer. Without any restriction we consider the jth layer. Because $V_j(\vec{r})$ is zero outside this range and because both Green's functions $G(E,\vec{k}_{||};\vec{r},\vec{r}\,')$ and $G^{e(j)}(E,\vec{k}_{||};\vec{r},\vec{r}\,')$ obey the two-dimensional Bloch theorem, the integral in Eq. (9) covers only one unit cell of this layer. Therefore, we need to know $G^{e(j)}$ only within this region. Because the potential energy of $G^{e(j)}$ is constant in this region, the empty layer Green's function can be expanded in terms of spherical Bessel and Hankel functions. As a consequence Eq. (9) reduces to the calculation of the scattering of a free electron at a localized potential. This is a well-known problem.[19] Therefore, we are left with the evaluation of Eq. (10) for $\vec{r}$ and $\vec{r}\,'$ within the range of the jth layer. This means that we have to calculate the reflection of the Green's function G^0 at the two boundaries of $\sum_{i=0}^{j-1}V_i(\vec{r})$ and of $\sum_{i=j+1}^{\infty}V_i(\vec{r})$ and the multiple scattering between them. We emphasize that the knowledge of $G^{e(j)}$ outside the empty region (i.e., the jth layer) is not needed. If we introduce reflection operators

$$R_j^{-}(E,\vec{k}_{||})=G^0(E,\vec{k}_{||})\left[\sum_{i=0}^{j-1}V_i\right]\left[1-G^0(E,\vec{k}_{||})\left[\sum_{i=0}^{j-1}V_i\right]\right]^{-1} \tag{11a}$$

and

$$R_j^{+}(E,\vec{k}_{||})=G^0(E,\vec{k}_{||})\left[\sum_{i=j+1}^{\infty}V_i\right]\left[1-G^0(E,\vec{k}_{||})\left[\sum_{i=j+1}^{\infty}V_i\right]\right]^{-1} , \tag{11b}$$

Eq. (10) reads

$$G^{e(j)}(E,\vec{k}_{||})=(1+R_j^+ +R_j^- +R_j^+R_j^- +R_j^-R_j^+ +\cdots)G^0(E,\vec{k}_{||}) \tag{12a}$$

$$=[1+R_j^+(1-R_j^-R_j^+)^{-1}+(1-R_j^-R_j^+)^{-1}R_j^- +R_j^+(1-R_j^-R_j^+)^{-1}R_j^- +(1-R_j^-R_j^+)^{-1}R_j^-R_j^+]G^0(E,\vec{k}_{||}) . \tag{12b}$$

For the convenience of shorter notation Eqs. (11) and (12) are written in the operator formulation. We note that the particular ordering of the reflection processes in Eq. (12b) allows us to treat the multiple scattering exactly.[16] In the actual calculation Eq. (12b) is evaluated in a plane-wave basis $\exp[i(\vec{k}_{||}+\vec{g},k_{g_z})\cdot\vec{r}]$ because then the matrices of R^+, R^-, and G^0 are finite in a good approximation and the method to calculate those reflection matrices for a finite or infinite number of layers is well established in the LEED theory.[19] The same calculation is also possible for a bulk layer. Then both reflection matrices R^+ and R^- describe the reflection at a semi-infinite crystal.

B. Final state

The method to calculate the final state of angular-resolved photoemission will not be discussed in detail as this follows closely the approach of LEED. The particular boundary condition of this wave function was noted above. Accordingly the time-reversed final state is calculated as an incoming plane wave which is scattered at the semi-infinite crystal. The difference compared to the standard LEED problem arises because in photoemission we are not interested in the asymptotic behavior of this wave function (far away from the crystal), but we need the wave function inside the crystal close to the nuclei. For this calculation as well as for the evaluation of the photocurrent we use the formulation of Pendry.[17]

C. Choice of parameters

We start from the electronic ground state of a Pd crystal which we take from the self-consistent band-structure calculation of Moruzzi *et al.*[20] This potential is of the muffin-tin form. Therefore, the splitting of the crystal into nonoverlapping layers [see Eq. (8)] is obvious. We use the same potential for all layers from the bulk to the surface. The surface barrier which connects the vacuum with the surface atomic layer is approximated by a step function. This potential does not account properly for the rearrangement of electronic charge at the surface, but it is a reasonable approximation for the questions addressed in the present study. We now discuss a modification of the electronic ground-state potential which is important for the calculation of the photocurrent. Figure 1 shows schematically the potential at a crystal surface. The effective one-particle potential, $V_{\text{eff}}(\vec{r})$, is built from two contributions. There is the classical electrostatic potential $V_{\text{es}}(\vec{r})$ of the nuclei and the electronic charge density, and secondly there is the quantum-mechanical contribution, $V_{\text{xc}}(\vec{r})$ describing exchange and correlation. The height of the potential barrier at the surface is denoted by V_0 and the work function is Φ. This potential holds for the electronic ground state of the crystal, i.e., for electron states below the Fermi level. The Green's function in Eq. (3) should, however, describe the hole created by the photoexcitation process. For Pd no indications of strong hole-hole correlation effects have been observed.[5] Therefore, the potential entering the Green's function calculation is modified only insignificantly: the main aspect not included in the ground-state potential is the finite lifetime of the hole. This can be treated in a phenomenological way by adding a small imaginary part Γ to the potential. We use a linear increase with $\Gamma(E_F)=-0.1$ eV and $\Gamma(E_F-4\text{ eV})=-0.5$ eV. The main consequence is a broadening of the peaks in the photoemission spectrum: a discrete level at the Fermi energy gets a full width at half maximum of 0.2 eV, and a level at E_F-4 eV gets a width of 1 eV.

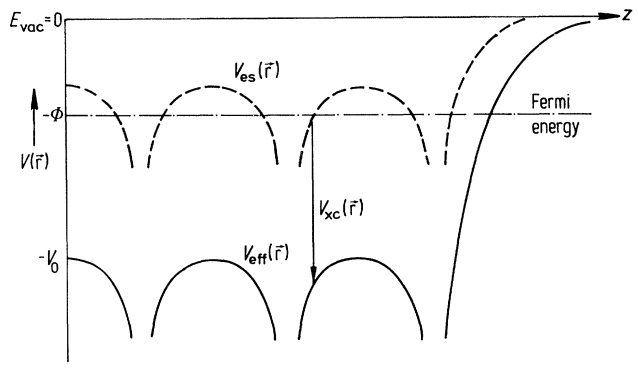

FIG. 1. Schematic figure of the effective single-particle potential $V_{\text{eff}}(\vec{r})$ (solid line) and the electrostatic potential $V_{\text{es}}(\vec{r})$ (dashed line) normal to a solid surface. $V_{\text{xc}}(\vec{r})$ is the exchange-correlation potential, V_0 the inner potential, and Φ the work function.

Whereas the modification of the ground-state potential is not very important in the present study for the initial states, it is significant for the wave function of the final state. For unoccupied states the exchange-correlation interaction is expected to decrease with increasing energy. In the classical limit, i.e., $E\rightarrow\infty$, it is zero and we are left with the electrostatic potential. Furthermore, the inelastic electron-electron interactions have to be considered. They determine the small escape depth of the photoelectron and thus the high surface sensitivity of ARUPS. Both effects, the decrease of V_{xc} and the inelastic interactions, are not independent of each other and they should be described by replacing the exchange-correlation potential, $V_{\text{xc}}(\vec{r})$, by an energy-dependent complex nonlocal self-energy $\Sigma(E,\vec{r},\vec{r}')$.[21] Since the detailed behavior of $\Sigma(E,\vec{r},\vec{r}')$ is not known for a real surface, we use an approximation which is common in LEED intensity calculations. Thus we account for these effects by using a complex optical

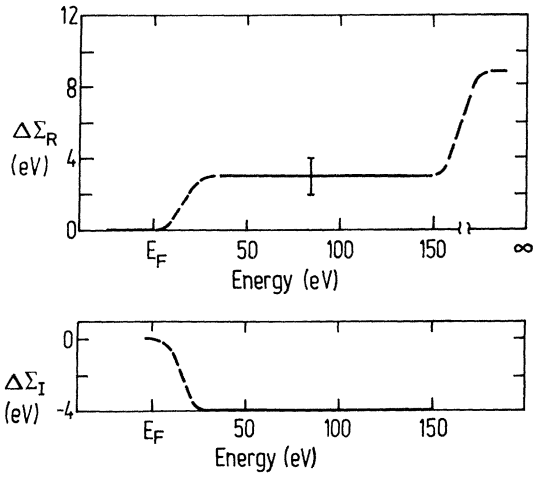

FIG. 2. Energy dependence of the real and imaginary part of the self-energy $\Sigma(E,\vec{r})$ [see Eq. (13)], as determined by LEED (Ref. 22).

potential:

$$\Sigma(E,\vec{r})=V_{xc}(\vec{r})+\Delta\Sigma(E)\theta(z-z_0)\ . \tag{13}$$

θ is the step function which is zero in the vacuum region ($z>z_0$) and unity otherwise. The order of magnitude of $\Delta\Sigma(E)$ has been estimated from a LEED analysis for the clean and adsorbate covered Pd(100) surface.[22] Approximately, this result should hold for other Pd surfaces as well. Figure 2 shows the result of this analysis. Between E_F+30 eV and E_F+150 eV the real part of $\Delta\Sigma(E)$ is approximately constant, $\Delta\Sigma_R(E)=3\pm1$ eV. The imaginary part is estimated as $\Delta\Sigma_I(E)=-4$ eV. For the He I ($\hbar\omega=21.2$ eV) photoemission the energy of the photoexcited electron is just in the middle between the Fermi energy and the lower energy of this LEED analysis.

Therefore, we have chosen

$$\Delta\Sigma_R(E)=+1.5\text{ eV}\ , \tag{14a}$$

$$\Delta\Sigma_I(E)=-2\text{ eV}\ . \tag{14b}$$

The other parameters of the calculation are concerned with the height and position of the surface barrier and with the basis set. As mentioned above the surface barrier is approximated by a step function. Its position is just in front of the muffin-tin potentials of the surface layer. For the electronic ground state its height V_0 (see Fig. 1) is determined from the calculated Fermi energy (6.8 eV) above muffin-tin zero[20] and from the experimentally determined work function [$\Phi=5.6$ eV for Pd(111) (Ref. 23)]. This adds up to $V_0=12.4$ eV. Concerning the plane-wave basis set it was sufficient to take between 19 and 22 reciprocal lattice vectors into account (the actual number depends on the value and direction of $\vec{k}_{||}$). In the angular momentum representation we include spherical waves up to $l=4$.

The vector potential is calculated from the Fresnel formulas. We use the value inside the crystal. The dielectric constant at $\hbar\omega=21.2$ eV is taken from an experimental analysis which gave $\epsilon_1=0.71$ and $\epsilon_2=1.45$.[24]

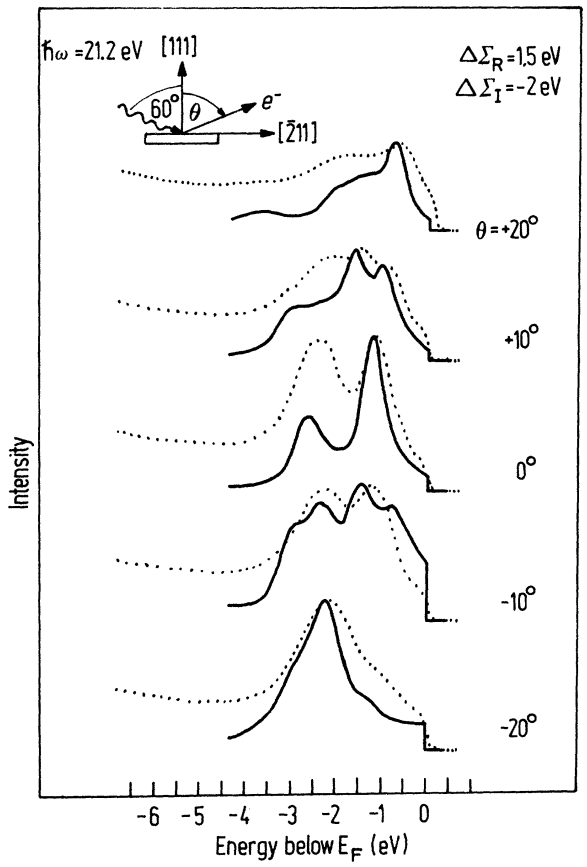

FIG. 3. Theoretical angle-resolved photoemission spectra (solid line) and experimental results of Dahlbäck *et al.* (Ref. 25) (dashed line) for the Pd(111) surface. The geometry is shown in the inset.

III. RESULTS

The most sophisticated approach for analyzing ARUPS is the one-step theory [see Eq. (3)]. Unfortunately this approach is quite elaborate and the comparison of those calculated photoemission *spectra* with the experimental results allows no direct insight into the nature of the photoemission process. In this section we discuss the calculations of photoemission, i.e., final-state, initial-state Green's function, and photoemission spectra for the clean Pd(111) surface. In Sec. III A we compare these calculated spectra to experimental results. In Secs. III B and III C we then analyze the initial-state Green's function and final-state band structure in order to elucidate the validity of various models which are commonly used for the analysis of ARUPS.

A. One-step approach of photoemission

We start our study of various models for the interpretation of ARUPS with a discussion of theoretical photoemission spectra which are calculated within the one-step approach [i.e., Eq. (3)]. Figure 3 shows the calculated re-

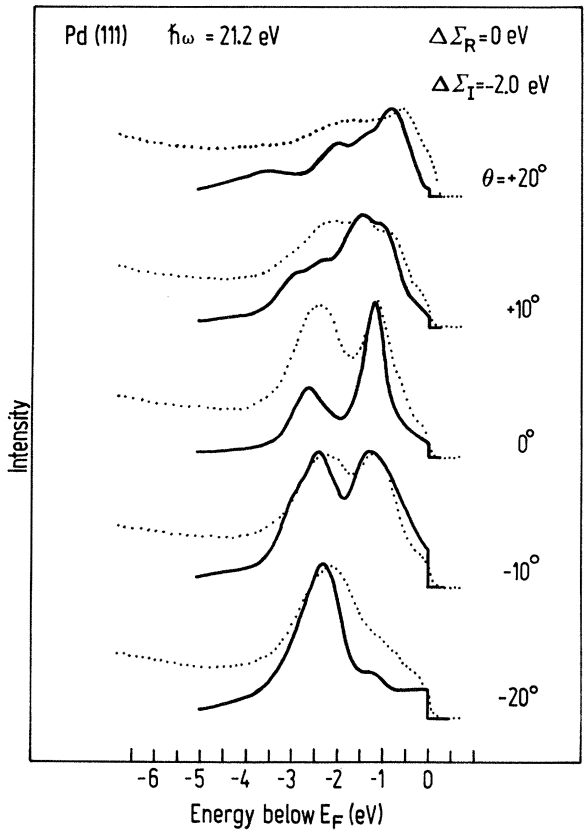

FIG. 4. Same as Fig. 3, but for $\Delta\Sigma_R = 0$.

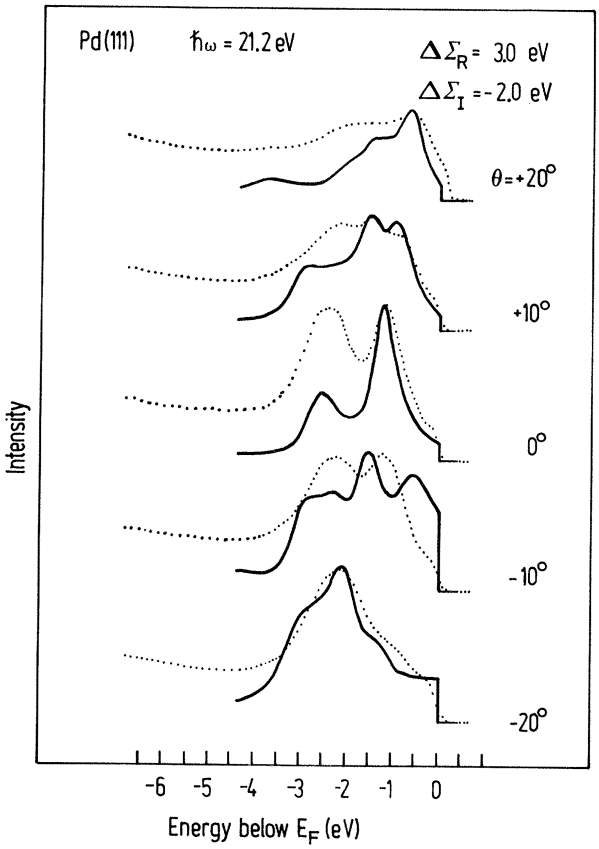

FIG. 5. Same as Fig. 3, but for $\Delta\Sigma_R = +3$ eV.

sults for the Pd(111) surface in comparison to the experimental data of Dahlbäck and co-workers.[25] The light is unpolarized and incident at a polar angle $\theta_{\hbar\omega} = 60°$. The azimuth is in the $[2\bar{1}\,\bar{1}]$ direction. Thus the light beam lies in the (110) plane. Also the emitted electrons are detected in this plane.

The agreement between theory and experiment is generally good, both for the energies of structures and for the intensities. In particular the characteristic change in the spectra from $\theta = +20°$ to $\theta = -20°$ is well reproduced by the theory. We therefore conclude that our description of the Pd crystal and its surface accounts well for the electronic structure of the initial and final states and the optical transition matrix elements.

Nevertheless, we also see some deviations between the theoretical and experimental spectra. There are several reasons which could cause these differences. At first we note that the spin-orbit coupling is not included in the calculations. This approximation affects the energies by up to 0.4 eV and it also changes the hybridization of wave functions and therefore the relative intensities in the photoemission spectra. Another uncertainty is the treatment of the incident light. In our approach the electric field is assumed to be constant over the region where the optical excitation takes place. We note that a better description is not known for a realistic surface, but a different approach will affect the relative intensities of peaks. Finally, we emphasize the uncertainty in energies and intensities due to the self-energy $\Sigma(E,\vec{r})$. We recall that the correct behavior of this function is not known for a realistic surface. The choice used in the calculations of Fig. 3 (see Sec. II) is only a reasonable first approximation. In order to test the influence of the self-energy on calculated photoemission spectra we show in Figs. 4 and 5 two other choices of $\Sigma(E,\vec{r})$. In Fig. 4 we neglect the change in the real part of the potential, i.e., we set $\Delta\Sigma_R = 0$. And in the calculations of Fig. 5 we have used $\Delta\Sigma_R = +3$ eV, which is the value determined for the higher energies of LEED.[22] Comparing these results and those of Fig. 3 we see a clear dependence of the peak energies and intensities on $\Delta\Sigma_R$. The comparison with the experimental spectra, contained in each of the figures, does not favor the one or the other choice. The value of $\Delta\Sigma_R = +1.5$ eV is only a reasonable compromise. Calculations with different choices of $\Delta\Sigma_I$ from -1 to -4 eV show differences of the same order of magnitude. The value of $\Delta\Sigma_I = -2$ eV turned out to be the best compromise.

Despite these uncertainties we conclude that the overall agreement between experiment and theory is good. Therefore, we can now perform a detailed analysis of the calculated photoemission spectra in order to test the various models which are commonly used for the interpretation of experimental spectra.

B. $\vec{k}_{\parallel}$-resolved density of states

One model for the interpretation of ARUPS emphasizes that the wave-vector component k_z of the photoelectron is

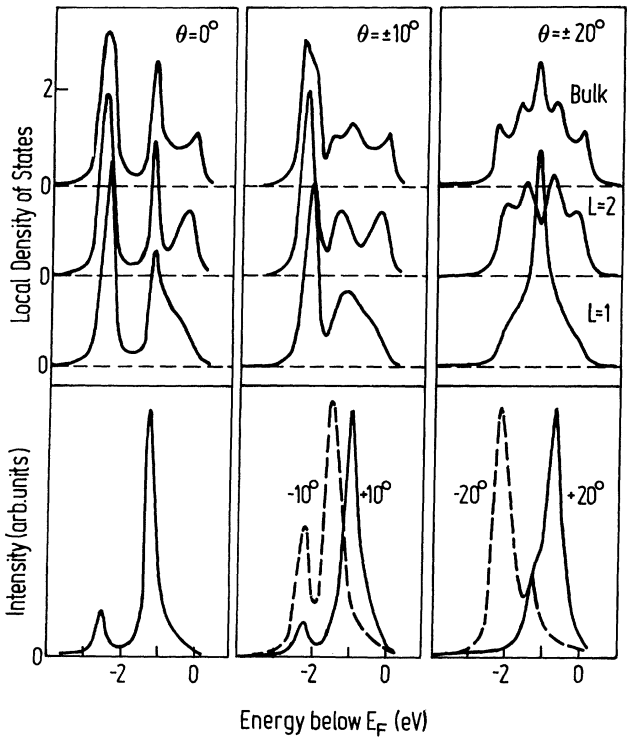

FIG. 6. $\vec{k}_{||}$-resolved local densities of states per atom and eV for Pd(111). Only states which are symmetric with respect to the (110) plane are considered. The three top rows show results for the bulk layer, the second and the first surface layer. The bottom row displays the corresponding angle-resolved photoemission spectra for *s*-polarized light. The geometry is shown in the inset of Fig. 3.

not conserved in the photoemission process. Further it is assumed that a photoemission spectrum can be interpreted as an image of the $\vec{k}_{||}$-resolved density of states (DOS). This model accounts well for the emission from intrinsic surface states and from adsorbate induced states. For clean transition metals a significant high density of surface states has been reported.[10,11] Therefore, it might be expected that the $\vec{k}_{||}$-resolved density of these states at the surface dominates the photoemission.[13] Such a model has also been used for the interpretation of ARUPS from GaAs.[12]

In order to determine the quality of this approach we compare theoretical angle-resolved photoemission spectra for Pd(111) with the corresponding DOS. We emphasize that both are calculated from the same Green's function $G(E,\vec{k}_{||};\vec{r},\vec{r}')$. We use the same geometry as in Fig. 3. Thus $\vec{k}_{||}$ points in the $[2\bar{1}\,\bar{1}]$ direction, i.e., it lies in the (110) plane which is a mirror plane of the semi-infinite crystal. As a consequence the wave functions are either symmetric or antisymmetric with respect to this plane. The dipole-selection rules then determine that *s*-polarized light can only excite electrons from antisymmetric initial states and *p*-polarized light excites only from symmetric initial states. Therefore, we compare the photoemission spectra and DOS for symmetric and antisymmetric states separately. The results are shown in Figs. 6 and 7. For convenience of a clearer discussion we have introduced a little modification compared to the calculations of Fig. 3: We have neglected the energy dependence of the hole lifetime and use $\Gamma=-0.1$ eV for the whole valence band. This gives sharper structures and thus allows a clearer comparison.

The upper parts of Figs. 6 and 7 display the local densities of states for a layer in the bulk and for the first and second layers at the surface. These DOS are identical for both directions ($\vec{k}_{||}$ and $-\vec{k}_{||}$) because of time reversal symmetry. The lower part of these figures shows the corresponding photoemission spectra for $+\theta$ and $-\theta$. The spectra are clearly different for both directions of emission. Similarities between certain spectra and the layer DOS turn out to be incidental. A closer inspection of those cases shows that the positions of the maxima do not coincide exactly. As both results are obtained from the same Green's function we can conclude that the $\vec{k}_{||}$-resolved density of states cannot explain the angle-resolved photoemission.

Before continuing the discussion of other models, we like to compare our results to those of the self-consistent pseudo-potential calculation of Louie.[10] At first we note that for the bulk both calculations are self-consistent and they agree in fact to within an accuracy of ± 0.2 eV. For the surface our calculation is not self-consistent. Nevertheless, the agreement between our results for surface states or resonances and surface DOS with those of Louie is of the same quality as that of the bulk layer.[26]

C. Direct transition model

In the direct transition model it is assumed that k_z is a good quantum number and is conserved in the optical excitation. A photoemission spectrum is then interpreted in terms of direct transitions between the bulk energy bands $E(\vec{k})$. Because $\vec{k}_{||}$ is determined directly by the experimental geometry [see Eq. (2)], the initial- and final-state bands should be considered as a function of k_z. When the final-state bands are shifted down by the photon energy, the cross points with the occupied bands determine the energies of possible transitions. Several calculations of angle-resolved photoemission spectra have been performed in this model, i.e., the initial and final states are calculated for the same bulk ground-state potential and the transition matrix elements are evaluated between Bloch states.[6,7] Obviously the surface is completely neglected and also a complex self-energy has not been considered so far.

To test this model we have calculated the initial- and final-state band structure by using the ground-state potential. Figure 8 displays these results $E(k_z)$ for $\vec{k}_{||}$ corresponding to $\theta=20°$ [see Eq. (2)]. The comparison with the photoemission spectrum shows that there is no correlation between the direct transitions and the photoemission spectrum. The final-state band structure in Fig. 8 (dashed line) includes already the real part of the self-energy, $\Delta\Sigma_R=1.5$ eV. This gives rise to a constant shift of these bands. If this shift were neglected, the discrepancy between the direct transition model and the photoemission

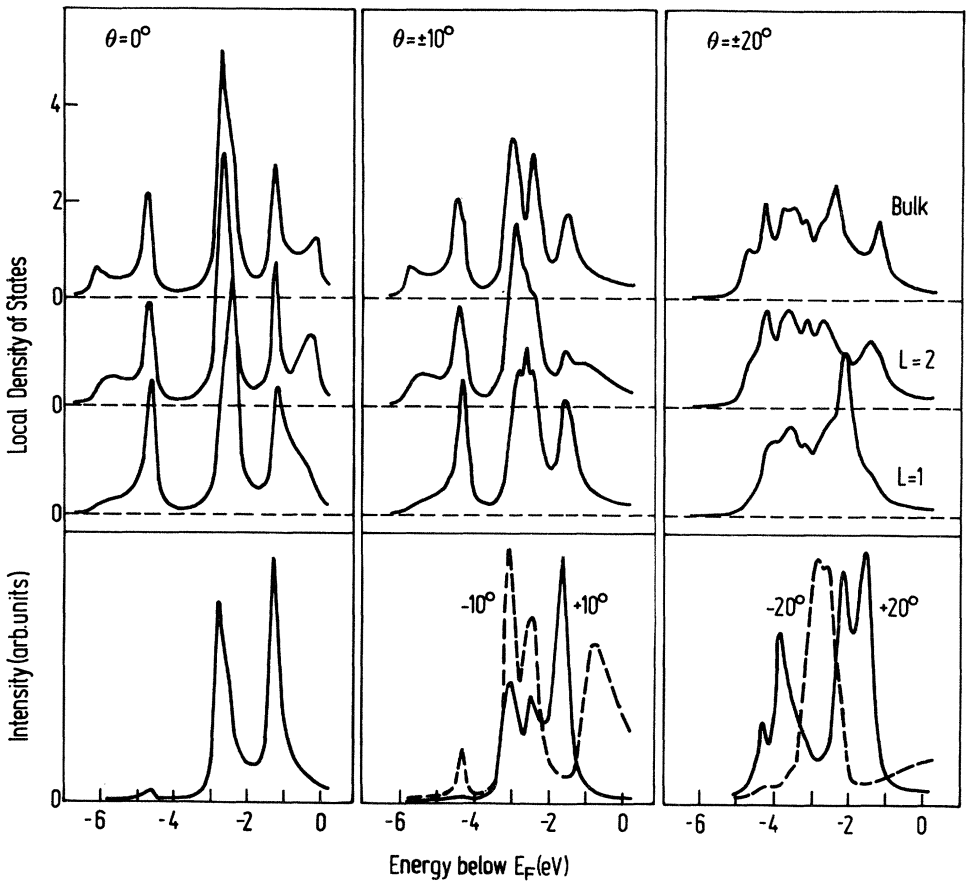

FIG. 7. Same as Fig. 6, but for states which are antisymmetric with respect to the (110) plane. The photoemission spectra are for p-polarized light.

spectra would be even larger. Thus the initial- and final-state band structure of Fig. 8 are calculated for the real potential, i.e., $\Delta\Sigma_I=0$. In contrast, in the photoemission spectrum a complex self-energy is taken into account (see Sec. II) at least in a crude first approximation. We show below that if the influence of the imaginary part of $\Sigma(E,\vec{r})$ is included in the band-structure calculation, then the direct transition model gives a good description of peak positions in ARUPS.

Figure 9 shows the influence of a complex self-energy on the band structure. At first (left part of Fig. 9) we consider the ground-state potential, thus setting $\Sigma(E,\vec{r})=V_{xc}(\vec{r})$. We note that in general also bands with complex wave vector are possible even for a real potential.[27] For bulk calculations these bands have no physical meaning as their wave functions are not normalizable. But their relevance arises for the surface calculations where they should be included for the representation of localized wave functions. Therefore, also bands with complex k_z are included. Owing to the periodicity parallel to the surface no localization is possible with respect to the x,y coordinates, and $\vec{k}_{||}$ has to be real. We show results for $\vec{k}_{||}=0$ (relevant to normal emission) and only bands with wave functions which remain unchanged under symmetry operations of the surface. Other wave functions have a node at the surface normal and thus cannot carry current normal to the surface. In the left band structure of Fig. 9 we see a s-p—derived band (labeled A) with a dispersion similar to that of a free electron. At about 18 eV this band is crossed by a flat f band leading to a small hybridization gap. Below 8 eV at L we see the top of a 6.5-eV gap and above 22 eV at Γ there is another gap. The size of these gaps reflects the significance of the interaction of electrons with the lattice. The broken lines give the bands with complex k_z. These bands are doubly degenerate. Only states with $|\mathrm{Im}k_z| \leq 0.3$ Å^{-1} are considered. When we take into account the complex self-energy of Eqs. (13) and (14), the band structure is changed significantly (right part of Fig. 9). The main modifications are:

(i) the degeneracy of the complex bands with $\pm\mathrm{Im}k_z$ is removed;

(ii) the real bands get a nonzero imaginary part of k_z;

(iii) the gaps in the band structure are closed.

Thus the s-p—derived band (A) shows a dispersion practically identical to a free-electron parabola and its imaginary part is nearly constant. The flat f band has disappeared and the two bands (B and C), which emerged from it (and several other complex bands of the real potential) have got an $\mathrm{Im}k_z$ at least twice as large as that of band A.

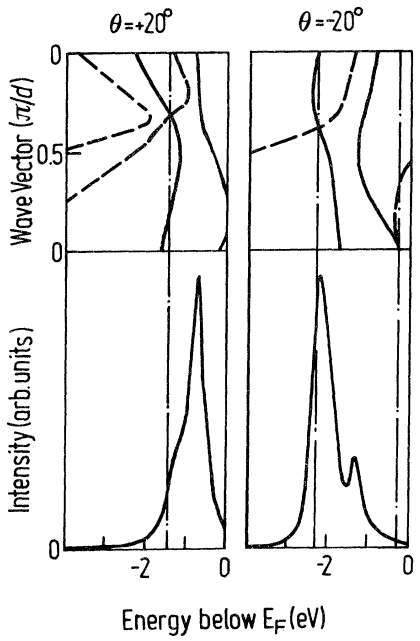

FIG. 8. Direct transition model for two angles of emission. Top: band structure of the real potential, i.e., $\Delta\Sigma_I=0$, for initial (solid line) and final states (dashed line). The latter are shifted down in energy by $\hbar\omega=21.2$ eV. Bottom: Calculated photoemission spectra for unpolarized light. The geometry is shown in the inset of Fig. 3. The distance between two layers parallel to the surface is $d=2.27$ Å.

The above discussion shows that the influence of a complex self-energy on the band structure can indeed be significant. Based on an experimental analysis of ARUPS on aluminum, this has been also shown recently by Levinson, Greuter, and Plummer.[28] Therefore, we include the complex self-energy for a further test of the direct transition model. This is displayed in Fig. 10. The band structure $E(k_z)$ in these figures is calculated at a wave vector $\vec{k}_{||}$ according to the photoemission parameters [see Eq. (2)], and the unoccupied states are shifted down by the photon energy. In the middle row we show the complex band structure which is calculated with the same $\Sigma(E,\vec{r})$ as the photoemission. The top row shows the bands for the real potential ($\Delta\Sigma_I=0$) for comparison. Only certain bands need to be considered: Final-state bands with a sign of $\mathrm{Im}k_z$ such that the wave functions increase into the solid are not meaningful and states which decay too fast, i.e, with $\mathrm{Im}k_z \geq 0.3$ Å^{-1} are neglected as well. Further the group velocity of the final states has to point towards the vacuum region. We only discuss results for *s*-polarized light, but those for *p*-polarized light show qualitatively the same behavior. Figure 10 shows that the direct transition model works when the influence of $\Sigma(E,\vec{r})$ is included. We also not that only one final-state band, namely that labeled as *A*, contributes to the photoemission. A comparison with the real potential band structure shows that this band is derived from the nearly free-electron, or *s-p* band. This band couples best to the plane wave in the vacuum measured by the detector. Transitions into other bands

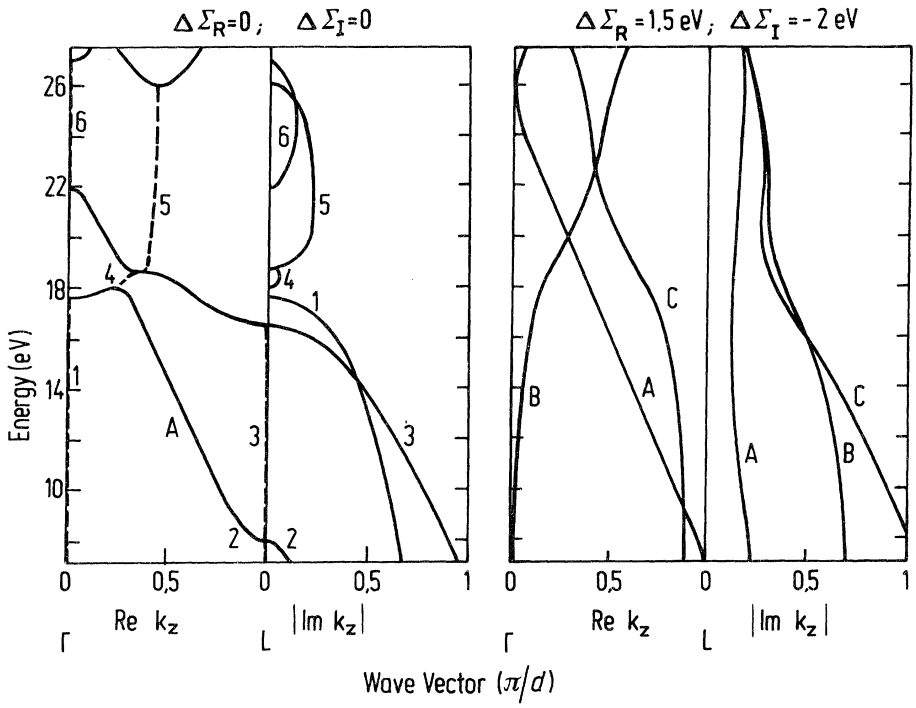

FIG. 9. Complex band structure for Pd along ΓL. Only states relevant for normal emission in ARUPS are considered [no node in the (111) direction]. Left: Calculated for the self-consistent ground-state potential of Ref. 20. Right: Calculated for a modified ground-state potential [see Eqs. (13) and (14)]. The distance between two layers parallel to the surface is $d=2.27$ Å.

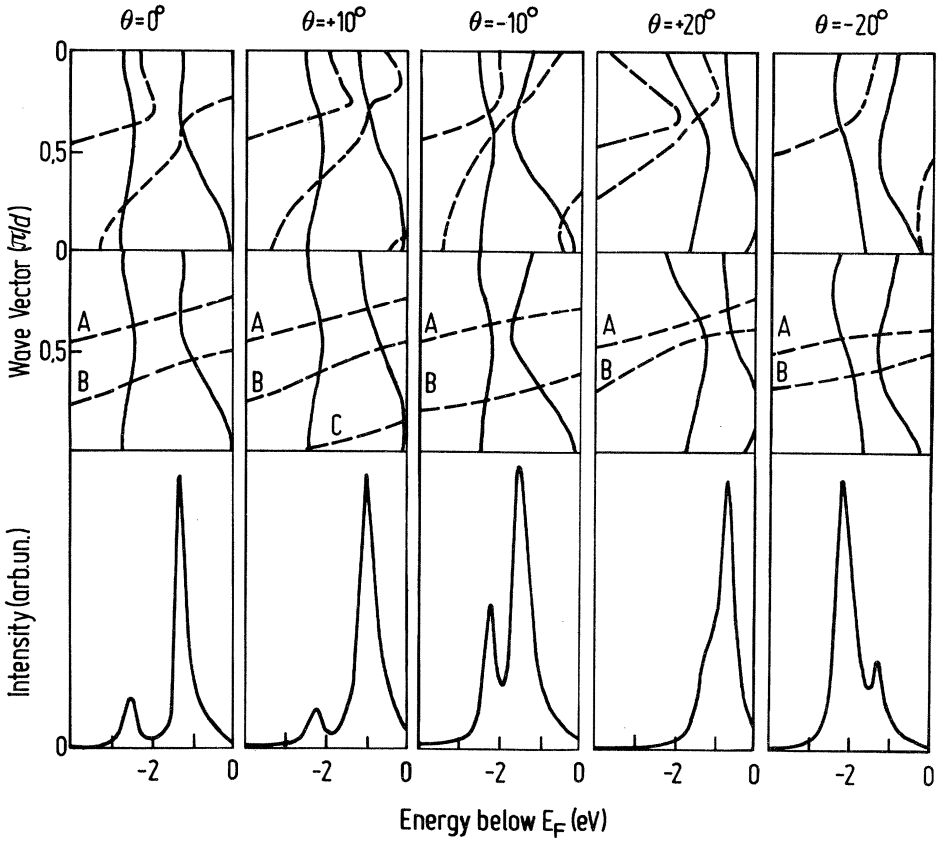

FIG. 10. Direct transition model for ARUPS from Pd(111). Top row: Band structure of initial (solid lines) and final states (dashed lines). The latter are shifted down in energy by 21.2 eV. Calculated for the real potential, i.e., $\Delta\Sigma_I=0$. Middle row: Same as top, but final states are calculated for a modified potential [see Eqs. (13) and (14)]. Bottom row: Calculated photoemission spectra. The geometry is shown in the inset of Fig. 3. The distance between two layers parallel to the surface is $d=2.27$ Å.

but A are found to be negligible. We emphasize however that the free-electron-like dispersion of band A does not imply a free-electron wave function. The wave function is significantly more complicated than a single plane wave. Similar results for Cu have been reported by Jepsen.[15]

The energy or wave-vector uncertainty due to the complex energy has only little effect with respect to the accuracy of energies predicted by the direct transition model. In various calculations for s- and p-polarized light and several polar and azimuthal angles the discrepancy between the energies of direct transitions and of peaks in the photoemission was always less than 0.2 eV.

IV. SUMMARY

In this paper we reported KKR Green's-function calculations for the electronic structure of a semi-infinite Pd crystal. The results agree with those of the self-consistent pseudopotential calculations for a seven-layer Pd slab of Louie.[10] Further we have calculated the energy- and ıgle-resolved photoemission using the one-step theory of Pendry. The comparison with experimental data shows that the theory accounts for all main features and trends.

We have then concentrated on a discussion of various models commonly used for the analysis of ARUPS. Our approach is based on the fact that the one-step theory of photoemission should be able to confirm the one or the other model. The detailed analysis shows that the main structures in a photoemission spectrum can be understood in terms of a modified direct transition model where the influence of a complex self-energy, $\Sigma(E,\vec{r})$, is included in the calculation of the unoccupied bands. We have only considered a crude approximation of $\Sigma(E,\vec{r})$ and there is some hope that this might be sufficient in many applications. For a detailed analysis of ARUPS, or at lower final-state energies, a better treatment might be important. No such calculation has been attempted.

ACKNOWLEDGEMENT

This work has been supported in part by the Deutsche Forschungsgemeinschaft.

[1]*Photoemission and the Electronic Properties of Surfaces,* edited by B. Feuerbacher, B. Fitton, and R. F. Willis (Wiley, New York, 1978).

[2]M. Scheffler and A. M. Bradshaw, in *The Chemical Physics of Solid Surfaces and Heterogeneous Catalysis, Vol. II: Adsorption on Solid Surfaces,* edited by D. A. King and D. P. Woodruff (Elsevier, Amsterdam, 1983), p. 165.

[3]P. Thiry, D. Chandesris, J. Lecante, C. Guillot, R. Pinchaux, and Y. Pétroff, Phys. Rev. Lett. 43, 82 (1979).

[4]P. Heimann, H. Miosga, and H. Neddermeyer, Solid State Commun. 29, 463 (1979).

[5]F. J. Himpsel and D. E. Eastman, Phys. Rev. B 18, 5236 (1978).

[6]N. V. Smith, R. L. Benbow, and Z. Hurych, Phys. Rev. B 21, 4331 (1980).

[7]S. Holloway, D. E. Grider, and J. K. Sass, Solid State Commun. 40, 809 (1981).

[8]W. E. Spicer, Phys. Rev. 112, 114 (1958).

[9]F. J. Himpsel, Appl. Opt 19, 3964 (1980).

[10]S. G. Louie, Phys. Rev. Lett. 40, 1525 (1978).

[11]J. G. Gay, J. R. Smith, F. J. Arlinghaus, and T. W. Capehart, Phys. Rev. B 23, 1559 (1981).

[12]A. Mazur, J. Pollmann, and M. Schmeits, Solid State Commun. 42, 37 (1982).

[13]O. Bisi and C. Calandra, Surf. Sci. 83, 83 (1979).

[14]J. B. Pendry and D. J. Titterington, Commun. Phys. 2, 31 (1977).

[15]D. W. Jepsen, Phys. Rev. B 20, 402 (1979).

[16]K. Kambe and M. Scheffler, Surf. Sci. 89, 262 (1979).

[17]J. B. Pendry, Surf. Sci. 57, 679 (1976); J. F. L. Hopkinson, J. B. Pendry, and D. J. Titterington, Comp. Phys. Commun. 19, 69 (1980).

[18]I. Adawi, Phys. Rev. 134, A1030 (1964).

[19]J. B. Pendry, *Low Energy Electron Diffraction* (Academic, London, 1974).

[20]V. L. Moruzzi, J. F. Janak, and A. R. Williams, *Calculated Electronic Properties of Metals* (Pergamon, New York, 1978).

[21]L. Hedin and B. I. Lundqvist, in *Solid State Physics,* edited by F. Seitz, D. Turnbull, and H. Ehrenreich (Academic, London, 1969), Vol. 23.

[22]W. Berndt, R. Hora, and M. Scheffler, Surf. Sci. 117, 188 (1982).

[23]J. E. Demuth, Surf. Sci. 65, 369 (1977).

[24]C. Wehenkel (private communication).

[25]N. Dahlbäck, P. O. Nilsson, and M. Pessa, Phys. Rev. B 19, 5961 (1979).

[26]R. Hora, thesis, University of Dortmund, 1983 (unpublished).

[27]V. Heine, Proc. Phys. Soc. London 81, 300 (1963).

[28]H. L. Levinson, F. Greuter, and E. W. Plummer, Phys. Rev. B 27, 727 (1983).